

# Energy Dispersive XAFS: Characterization of Electronically Excited States of Copper(I) Complexes

Moniek Tromp,<sup>†,‡</sup> Andrew J. Dent,<sup>§</sup> Jon Headspith,<sup>⊥</sup> Timothy L. Easun,<sup>||</sup> Xue-Zhong Sun,<sup>||</sup> Michael W. George,<sup>||,¶</sup> Olivier Mathon,<sup>#</sup> Grigory Smolentsev,<sup>○</sup> Michelle L. Hamilton,<sup>||,¶</sup> and John Evans<sup>†,§,¶,\*</sup>

<sup>†</sup>School of Chemistry, University of Southampton, Southampton, SO17 1BE, U.K.

<sup>‡</sup>Catalyst Characterization, Catalysis Research Center, Chemistry, Technische Universität München, Lichtenbergstrasse 4, Garching bei München, Germany

<sup>§</sup>Diamond Light Source Ltd., Didcot, U.K.

<sup>⊥</sup>STFC Daresbury Laboratory, Warrington, U.K.

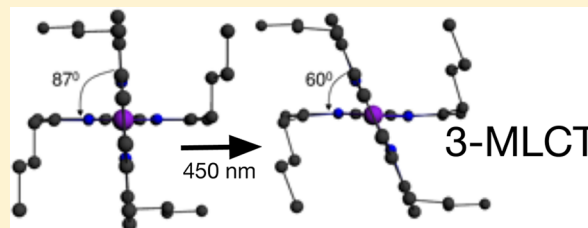
<sup>||</sup>School of Chemistry, University of Nottingham, Nottingham, U.K.

<sup>#</sup>European Synchrotron Radiation Facility, Grenoble, France

<sup>○</sup>Paul Scherrer Institute, Villigen, Switzerland

<sup>¶</sup>Research Complex at Harwell, Didcot, U.K.

**ABSTRACT:** Energy dispersive X-ray absorption spectroscopy (ED-XAS), in which the whole XAS spectrum is acquired simultaneously, has been applied to reduce the real-time for acquisition of spectra of photoinduced excited states by using a germanium microstrip detector gated around one X-ray bunch of the ESRF (100 ps). Cu K-edge XAS was used to investigate the MLCT states of  $[\text{Cu}(\text{dmp})_2]^+$  ( $\text{dmp} = 2,9\text{-dimethyl-}1,10\text{-phenanthroline}$ ) and  $[\text{Cu}(\text{dbtmp})_2]^+$  ( $\text{dbtmp} = 2,9\text{-di-}n\text{-butyl-}3,4,7,8\text{-tetramethyl-}1,10\text{-phenanthroline}$ ) with the excited states created by excitation at 450 nm (10 Hz). The decay of the longer lived complex with bulky ligands, was monitored for up to 100 ns. DFT calculations of the longer lived MLCT excited state of  $[\text{Cu}(\text{dbp})_2]^+$  ( $\text{dbp} = 2,9\text{-di-}n\text{-butyl-}1,10\text{-phenanthroline}$ ) with the bulkier diimine ligands, indicated that the excited state behaves as a Jahn–Teller distorted Cu(II) site, with the interligand dihedral angle changing from 83 to 60° as the tetrahedral coordination geometry flattens and a reduction in the Cu–N distance of 0.03 Å.



## INTRODUCTION

Photoexcitation of molecules has been of major interest for the last 30 years due to their potential applications in solar energy conversion and storage, chemical sensing, photocatalysis and molecular devices.<sup>1–6</sup> In this respect,  $[\text{Cu}^{\text{I}}(\text{NN})_2]^+$  diimine coordination complexes and their photochemical and photo-physical properties have been investigated in extensive detail, the first and significant contributions coming from the McMillin group.<sup>7–14</sup> These 3d transition metal systems are preferred over well-known ruthenium(II), rhenium(I), and osmium(II) systems, in that they are economically more viable.<sup>7,15–17</sup>

The structural aspects of ligands for long-lived excited states in solution, and thus more useful for photoinduced electron and energy transfer, have been investigated. In homoleptic Cu(I) polypyridine complexes, sufficiently bulky ligand substituents at the 2- and 9- positions were found to be required for luminescence, with their lifetimes being ligand, concentration and solvent dependent.<sup>18,19</sup>  $[\text{Cu}^{\text{I}}(\text{dmp})_2]^+$  ( $\text{dmp} = 2,9\text{-dimethyl-}1,10\text{-phenanthroline}$ ) is one of the most studied cuprous diimine compounds and its mechanism of generating

the MLCT state is generally accepted.<sup>7–14</sup> The  $\text{Cu}^{\text{I}}$  ground state has a  $d^{10}$  electron configuration, with a slightly distorted tetrahedral geometry ( $C_2$ ). Absorption of a visible photon promotes an electron from the  $\text{Cu}^{\text{I}}$  center to the dmp ligands (to one or spread over both as recently has been suggested), generating a Franck–Cordon MLCT excited state with a  $\text{Cu}^{\text{II}*}$  center. The  $\text{Cu}^{\text{II}*}$   $d^9$  center is susceptible to a Jahn–Teller distortion resulting in an MLCT excited state with flattened tetrahedral coordination. The large shift observed between absorption and photoluminescence is consistent with significant structural changes in the flattened MLCT excited state that either returns to the ground state via a radiative decay pathway or forms a pentacoordinate complex with strong Lewis basic solvents, resulting in exciplex quenching in the ligated MLCT state. Up until a few years ago, structural information on the MLCT state of  $[\text{Cu}^{\text{I}}(\text{dmp})_2]^+$  was mostly indirect and derived

**Received:** February 27, 2013

**Revised:** April 30, 2013

**Published:** May 29, 2013

from the strong correlation between accessibility of the copper center to the Lewis base and the luminescence lifetimes.<sup>12,20</sup>

In the last ten years, the group of Chen et al.<sup>21–23</sup> has developed and used time-resolved X-ray techniques to study these Cu(I) systems and confirm the formation of an exciplex using extended X-ray absorption fine structure (EXAFS) results and X-ray absorption near edge structure spectroscopy (XANES), providing direct evidence for a five-coordinate species (by coordination of a solvent molecule or counterion) upon excitation in both poorly coordinating toluene and strongly coordinating acetonitrile, with the observed interaction being stronger in the latter one. The X-ray absorption spectroscopy (XAS) pump–probe studies of photoexcited transition metal complexes, with pulsed laser pump and pulsed X-ray probe were performed using a scanning monochromator and a 100 ps time resolution arising from the electron bunch width of the synchrotron source (Advanced Photon Source). The technique is of great current interest, with major current developments being carried out at the APS<sup>24</sup> and SLS.<sup>25</sup> Each of these facilities utilizes a scanning monochromator maintained at fixed energy with a time series built up by repeat acquisitions at each point in a time and energy 2-dimensional grid, giving experimental acquisition times of up to 40 h (with a 1 kHz laser), for a good signal-to-noise spectrum.<sup>21,26</sup> Here, we present the first results obtained using an energy dispersive data acquisition approach.

The energy dispersive approach has two advantages. First, the X-ray beam is focused so that it interrogates only within the laser irradiated volume. Second, the multiplexing intrinsic to an energy dispersive measurement provides the entire XAFS spectrum synchronously, and so has the potential to significantly reduce the total acquisition time. This is provisional upon the following points:

- (i) The flux of the polychromatic beam for the bandwidth corresponding to the measured spectrum is not significantly less than that of the monochromatic beam.
- (ii) The gating and repetition rates of the detector are sufficiently fast.

This had been achieved for stopped flow experiments at ID24 with experiments on Cu complexes in solution on a millisecond time scale using CCD-based detectors.<sup>27</sup> Also, a high degree of linearity is required to successfully derive difference spectra between light-on and light-off. What is of final importance for energy dispersive experiments is the relatively high concentration of the species under investigation required, since experiments need to be performed in transmission mode, a factor which can clearly influence the type and properties of excited states.

In this paper the energy dispersive approach is demonstrated on the well-known  $[\text{Cu}^{\text{I}}(\text{dmp})_2]^+$  system as was described above and the XANES data obtained. In addition, a larger ligand system  $[\text{Cu}^{\text{I}}(\text{dbtmp})_2]^+$  (dbtmp = 2,9-di-*n*-butyl-3,4,7,8-tetramethyl-1,10-phenanthroline)<sup>7</sup> having a much longer lifetime compared to the dmp complex (i.e., 181 vs 1.8 ns in acetonitrile for degassed samples at 15.5 mM and 20 mM respectively) was investigated.

## ■ EXPERIMENTAL SECTION

**Synthesis of Cu Complexes.** The synthesis of the  $[\text{Cu}^{\text{I}}(\text{dmp})_2]\text{X}$  (dmp = 2,9-dimethyl-1,10-phenanthroline, X =  $\text{PF}_6$  and  $[\text{B}(\text{C}_6\text{F}_5)_4]$ ) and the  $[\text{Cu}^{\text{I}}(\text{dbtmp})_2]\text{Y}$  (dbtmp = 2,9-di-

*n*-butyl-3,4,7,8-tetramethyl-1,10-phenanthroline, Y = Cl) were carried out according to literature procedures.<sup>7</sup>

**Pump–Probe XAS Experiments.** The experiments were performed at the energy dispersive XAS beamline ID24 of the ESRF, Grenoble, France. Experiments were performed in the 4-bunch mode, with 10 mA per bunch (compared to uniform filling mode of 200 mA) giving  $\sim 10^7$  photons per single bunch in the bandwidth used in 100 ps with a 700 ns interval. A 10 Hz Quantel Brilliant Q-Switched Nd:YAG laser, with a pulse width of 3 ns (fwhm), was used. Laser excitation was performed at 450 nm, with an OPO power of 12 mJ per pulse. XAFS measurements, in transmission mode, with a Si(111) polychromator in a Bragg geometry, using a Ge microstrip detector (XH) consisting of 1024 elements on a 50  $\mu\text{m}$  pitch, which was rapid enough in its acquisition time to isolate an individual electron bunch by parallelization of the charge integrating preamplifiers (128 element XCHIPS).<sup>28</sup> The detector was time-windowed (500 ns integration time) around the electron bunch, achieving a better than 100 kHz repetition rate. Initial synchronization was achieved using a Hamamatsu S2383 silicon APD which was sensitive to X-ray and visible light linked to a fast oscilloscope. The ESRF machine clock signal (352.2 MHz) was used as a timing basis to trigger the XH detector, and the flashlamp and Q-switch of the laser to vary the delay between excitation and recording. The X-ray spot was tuned to 5 (horizontal)  $\times$  100 (vertical)  $\mu\text{m}$  and its center positioned 15  $\mu\text{m}$  from laser entrance window. Alternating light-on and light-off measurements were taken to minimize the effects of beam movement, and providing direct XAS difference-spectra. In this experiment we have focused the polychromator around the XANES area and no high quality long-range EXAFS data, suitable for analysis, has been obtained. The energy dispersive data, as obtained in absorption as a function of pixel number, i.e. position on the detector, was energy calibrated using a reference Cu foil.

Each differential spectrum presented in this paper is an average of 37 spectra, each spectrum obtained from 10 pairs of light-on and light-off recordings (i.e., 10 difference spectra) of 100 accumulations (i.e., an average of a 100 individual difference spectra) each. This employed the XMCD protocol previously described.<sup>29</sup> Each set of 10 pairs could be repeated at 10 min intervals, with total experimental time of  $\sim 2$  h.

The  $[\text{Cu}^{\text{I}}(\text{dmp})_2]\text{PF}_6$  and the  $[\text{Cu}^{\text{I}}(\text{dbtmp})_2]\text{Cl}$  were measured as 20 and 15.5 mM respectively in acetonitrile. The solutions were measured in a continuous flow cell with quartz windows for the laser excitation and pyrolytic graphite windows for the X-ray transmission perpendicular to that. The solutions were pumped continuously to refresh the solution from a large container to minimize sample oxidation and radiation damage. The cell path length was 3 mm for X-radiation that was located 15  $\mu\text{m}$  from the end of the quartz rod on the laser inlet.

**Geometry Optimization.** Structure optimization was performed using DFT implemented in ADF2010 package.<sup>30</sup> The core shells of all atoms (except hydrogen) were treated with the frozen core approximation.<sup>31</sup> The valence atomic orbitals were described by triple  $\zeta$  Slater-type basis set with one polarization function for Cu atoms and double  $\zeta$  basis also with one polarization function for other atoms. For the ground and flattened excited states, the geometry was restricted to the  $C_2$  point group and the structural optimization for exciplex was performed without any symmetry constraints. Geometry convergence was considered reached when the Cartesian

length changes less than 0.01 Å and Cartesian gradients fell below the threshold of 0.01 hartree/Å.

**XANES Calculations.** XANES calculations have been performed on the basis of Slater-type orbitals calculated self-consistently using ADF2010 package. Nonrelativistic spin-unrestricted calculations for singlet and triplet states of the complex were performed. A quadruple- $\zeta$  basis set of the Slater-type was used. Intensities of 1s-to-unoccupied states XAS transitions were calculated by integration of dipole transition matrix elements between 1s-originated MOs and unoccupied MOs. Integration has been performed on a 3D spatial cubic grid in close proximity to the absorbing Cu atom with 132651 points and 0.01 Å step size in each direction. Simulation of the XANES spectral region (~50 eV) requires integration for ~800 lowest unoccupied MOs. Finally, Lorentzian broadening of this discrete spectrum was performed using the energy-dependent arctangent model. This accounted for the finite mean free path of the photoelectron, the core hole lifetime broadening (2 eV), and the polychromator resolution 1.4 eV). The exchange-correlation potential with parametrization by Vosko, Wilk, and Nusair<sup>32</sup> calculated within local density approximation (LDA) was used.

## RESULTS AND DISCUSSION

**[Cu<sup>I</sup>(dmp)<sub>2</sub>]PF<sub>6</sub> (20 mM) in Acetonitrile.** The XANES experiments are performed at significantly higher concentration than conventional photophysical measurements. [Cu<sup>I</sup>(dmp)<sub>2</sub>]<sup>+</sup> is nonemissive under these conditions and we have therefore performed time-resolved transient absorption (TA) measurements at the higher concentration (20 mM in degassed acetonitrile). The spectra are displayed in Figure 1. Photolysis

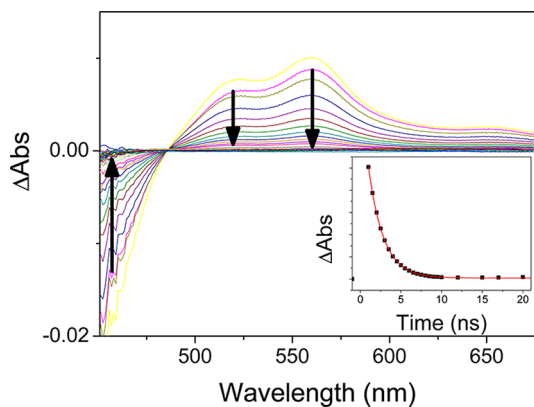


**Figure 1.** ns-TA spectra of [Cu(dmp)<sub>2</sub>](BARF) in CH<sub>3</sub>CN solution (20 mM) after 355 nm laser excitation. Inset: kinetics at 559 nm of the degassed sample, fitted to an exponential decay.

of [Cu<sup>I</sup>(dmp)<sub>2</sub>]<sup>+</sup>, as the BARF salt (BARF = [B(C<sub>6</sub>F<sub>5</sub>)<sub>4</sub>]<sup>-</sup>), at 355 nm clearly leads to bleaching of the ground-state absorption near 455 nm<sup>20</sup> and production of a lower energy transient peak at ~520 and 560 nm due to formation of the <sup>3</sup>MLCT excited state. The lifetime of this state under these conditions is 1.84 (±0.1) ns.

To perform the X-ray experiments, first the [Cu<sup>I</sup>(dmp)<sub>2</sub>]<sup>+</sup> ground state system was measured using normal ED-XAS. The spectrum is shown in Figure 2a and is identical to the Cu K-edge XANES as previously reported;<sup>23</sup> Figure 2b shows the acquired Cu K-edge XANES difference spectrum. Before excitation (-5 ns) and 5 ns after excitation, there is no

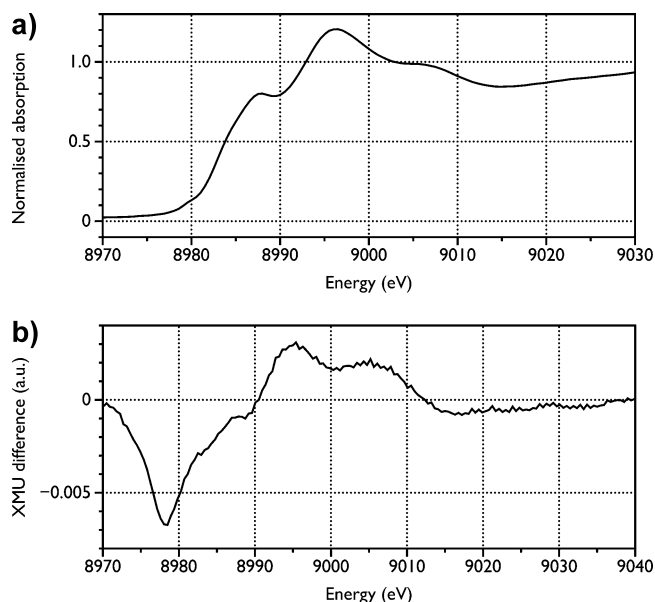


**Figure 2.** Cu K-edge XANES spectra for (a) [Cu<sup>I</sup>(dmp)<sub>2</sub>]PF<sub>6</sub> in CH<sub>3</sub>CN (20 mM). (b) Non-normalized differential spectrum (excited state-ground state XANES) for [Cu<sup>I</sup>(dmp)<sub>2</sub>]PF<sub>6</sub> in CH<sub>3</sub>CN (20 mM).

difference spectrum observed confirming the lifetime to be a maximum of 5 ns. At the laser excitation, however, a significant difference spectrum is observed, indicating the difference in species between ground state and after activation (excited state species). By comparison of the obtained data with the data as presented by L. X. Chen,<sup>23</sup> reported then to require 40 h using the scanning approach, similar data quality has been derived and the same difference spectrum recorded. It has to be noted here however that recent upgrades at the APS<sup>33</sup> have reduced the acquisition time scale considerably, for similar Cu systems to the order of 1–2 h. Moreover, the experiments by Chen et al.<sup>23</sup> are performed at 2 mM Cu concentration, whereas a concentration of 20 mM was utilized to afford good ED-XAS data. The ~2 h data acquisition time in the energy dispersive approach as presented here is mainly limited by the laser frequency being 10 Hz. In the future, using a kHz laser, we should be able to reduce this to a few minutes total data acquisition at most.

**[Cu<sup>I</sup>(dbtmp)<sub>2</sub>]Cl (15.5 mM) in Acetonitrile.** This complex contains a bulkier ligand system, retaining the 2,9-substitution of the dmp complex but extending the methyl groups to butyl chains. This substitution restricts deactivation of the excited state by restricting additional coordination to the metal center, meaning that the luminescence lifetime of [Cu<sup>I</sup>(dbtmp)<sub>2</sub>]<sup>+</sup> in deoxygenated acetonitrile at low concentration (typically ~10<sup>-5</sup> M) is reported to be 440 ns.<sup>7</sup> Given the significantly higher concentrations required for the X-ray experiments, we investigated the excited state behavior of the complex by transient absorption spectroscopy (Figure 3). Photolysis of [Cu<sup>I</sup>(dbtmp)<sub>2</sub>]<sup>+</sup> in acetonitrile at concentrations between 3 and 15.5 mM all afforded spectra with evidence of ground-state bleaching and production of transient peaks at 524 and 565 nm due to the formation of the <sup>3</sup>MLCT state. The lifetime of the 3 mM deoxygenated sample was found to be 299 ns, decreasing to 181 ns at 15.5 mM concentration, significantly shorter than the lifetime observed for the complex [Cu<sup>I</sup>(dtbp)<sub>2</sub>]<sup>+</sup> (1.9 μs, dtbp = 2,9-di-*tert*-butyl-1,10-phenanthroline) with *tert*-butyl groups ortho to the coordinated nitrogens.<sup>34</sup>

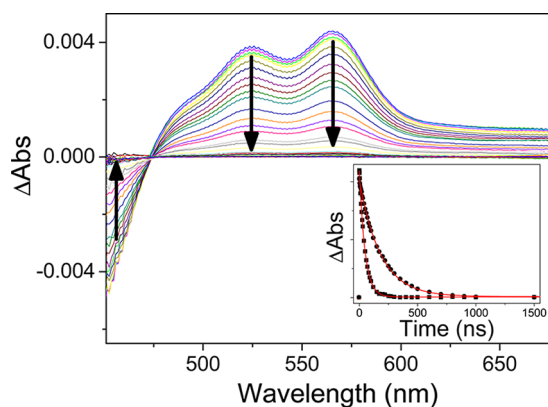


**Figure 3.** ns-TA spectra of  $[\text{Cu}(\text{dbtmp})_2]\text{Cl}$  in  $\text{CH}_3\text{CN}$  solution (15.5 mM) after 355 nm laser excitation. Inset: kinetics at 565 nm of the degassed (circles) and aerated (squares) sample, fitted to exponential kinetics (solid lines).

On oxygenating the sample by bubbling with air, the lifetime further decreases to only 48 ns at 15.5 mM, a full order of magnitude shorter than the low concentration, deoxygenated sample. This is entirely consistent with both self-quenching at high concentration and quenching of the excited state by oxygen in solution. Quenching by anion coordination has been reported for salts on  $[\text{Cu}(\text{dmp})_2]^+$ ,<sup>35</sup> but this effect is much reduced for  $[\text{Cu}(\text{Ph}_2\text{-phen})_2]^+$  ( $\text{Ph}_2\text{-phen}$  = 2,9-diphenyl-1,10-phenanthroline).<sup>36</sup> Chloride will subtend a larger cone angle at copper than acetonitrile and so the *o*-butyl groups in  $[\text{Cu}(\text{dbtp})_2]^+$  may resist its coordination, and so the nature of the concentration quenching is uncertain.

The ground state Cu K-edge XANES spectrum is very similar to that of the dmp complex, indicating a similar Cu(I) geometry. The difference spectrum between ground and excited states is presented in Figure 4.

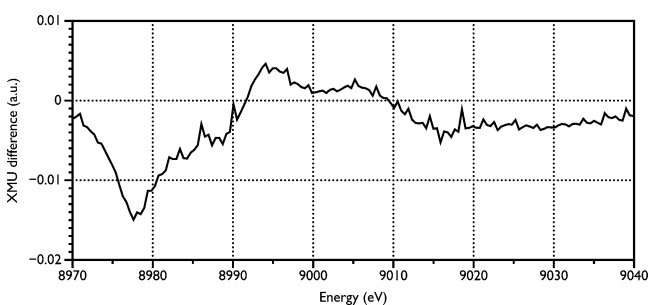


**Figure 4.** Cu K-edge XANES differential spectrum (excited state - ground state XANES) spectrum for  $[\text{Cu}^+(\text{dbtmp})_2]\text{Cl}$  in  $\text{CH}_3\text{CN}$  (15.5 mM).

The decay of the excited state of  $\text{Cu}^+(\text{dbtmp})_2^+$  was followed using the same EDE-pump-probe-XAFS method, measured at time-intervals of 10 ns, from 10 ns before laser excitation until 100 ns after laser excitation. The excited state signal clearly decreased over this time. To further quantify this, the areas of the first difference-XANES feature at  $\sim 8978$  eV were estimated by fitting a simple Gaussian between 8970 and 8990 eV, and plotting the area as a function of time, see Figure 5. The decay is shown to follow a first order exponential. The reason that the amount of excited state species at  $t = 0$  ns is nonzero is due to the fact that  $t = 0$  ns is measured during the laser pump, not at the end of the laser pump, where the amount

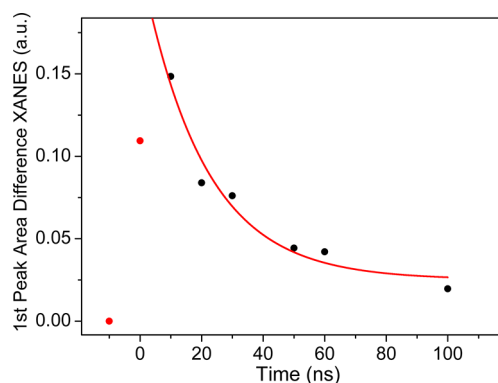


**Figure 5.** Differential spectra peak areas for  $[\text{Cu}^+(\text{dbtmp})_2]\text{Cl}$  complex in acetonitrile (15.5 mM) as a function of time, after excitation.

of excited state species is still rising. The lifetime (27 ns), as compared to Figure 3, indicates that there was considerable aeration of this solution.

**XANES Calculations.** These have been performed for two models of  $[\text{Cu}(\text{dbp})_2]^+$  ( $\text{dbp}$  = 2,9-di-*n*-butyl-1,10-phenanthroline) obtained using DFT optimization. The first model assumed only flattening distortions of the complex in the MLCT state while the second one corresponds to the exciplex state with the solvent molecule coordinating the metal ion. Formation of the exciplex for this complex with bulky groups that protect the metal center from the solvent might be considered less probable in comparison with  $[\text{Cu}^+(\text{dmp})_2]^+$ , since it requires significant reorganization of the ligand. The results for these two models are presented in Figures 6 and 7.

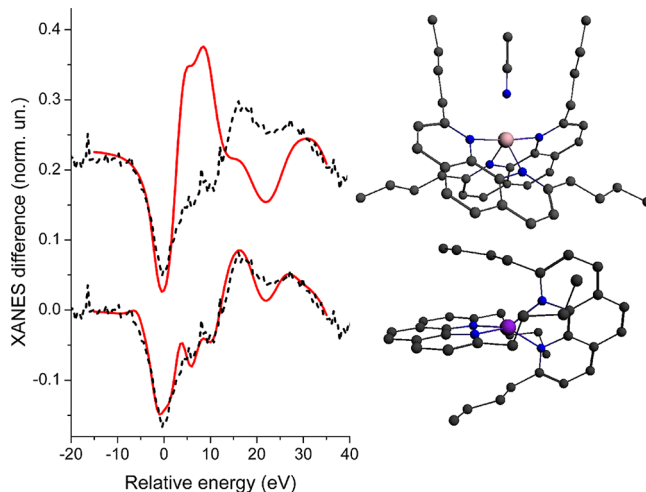


**Figure 6.** Theoretical difference spectra (red, solid) between Cu K-edge XANES of photoexcited and ground state  $[\text{Cu}^+(\text{dbp})_2]^+$ , compared to the experimental difference spectra of  $[\text{Cu}^+(\text{dbtmp})_2]^+$  (black, dashed). Calculations and corresponding models of the excited state are shown.

As one can see from Figure 7, the theoretical spectra of excited state species look very different. It can readily be seen from the difference spectra (Figure 6) that the agreement to experiment is much closer for the flattened structure. This model with flattening distortions has the same features as the ground state spectrum, but all of them are shifted to higher energy due to the changes of the core level as a result of the

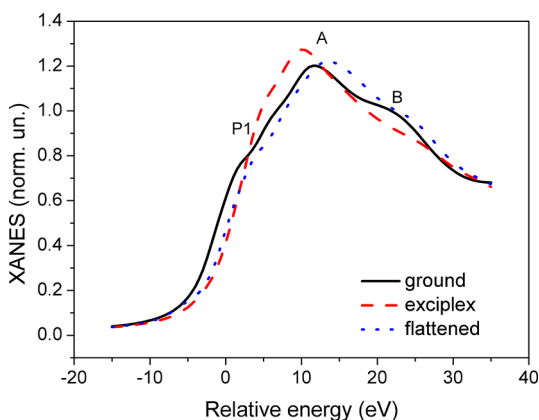


**Figure 7.** Theoretical XANES spectra of  $[\text{Cu}^{\text{I}}(\text{dbp})_2]^+$  in the ground state (black, solid) and for two models of the excited state with flattening distortions only (blue, dotted) and with exciplex complex (red, dashed) with significant rocking distortions.

oxidation state change. Moreover maximum A became more intense while peak B is less pronounced on transient oxidation of the Cu center. Peak P1 that was shifted in the previous work<sup>23</sup> now is in better agreement with the experiment. The use of molecular orbitals to calculate XANES allowed us to clarify the origin of this feature. In Figure 8, we have shown molecular orbitals (MOs) that contribute to the peak P1 in the ground state. They have significant p-character around Cu, oriented between the planes of the ligands and deformed by the butyl tails. Additionally  $\pi$  orbitals of C and N atoms of one of the ligands contributes to these MOs; a similar qualitative interpretation that the  $4p_z$  orbital of Cu produces a shoulder on the rising edge has been proposed by Solomon.<sup>37</sup> An analogous feature exists in the excited state spectrum for the flattened geometry. The negative peak in the difference spectrum within this model is related to the shift of the edge. On the contrary, in the exciplex model peaks P1 and B almost disappear. This trend was also observed for  $[\text{Cu}^{\text{I}}(\text{dmp})_2]^+$  calculations. The main maximum A calculated for the exciplex is too intense and shifted to lower energy, rather than shifted to higher energy according to the experimental data. As a result in the difference spectrum there is positive peak at relative energy 6–8 eV that is negative in the experiment. The model with flattening distortions gives good agreement with experiment. In the difference spectrum for this model one can note a very small positive peak that theory predicts at the relative energy -7 eV. This peak is related to the depopulation of the MO (Figure 6, bottom) with significant Cu d-character during the MLCT transition.

Thus, we can conclude that XANES has sufficient sensitivity to distinguish exciplex and flattening models for the MLCT excited states of Cu complexes. Good agreement between theory and experiment for the flattening model indicates that this model is the most probable for  $[\text{Cu}^{\text{I}}(\text{dbtmp})_2]^+$ . Within this model the angle between the ligands (angle between two planes formed by the N atoms of the corresponding ligands and the Cu atom) changes from  $83^\circ$  in the ground state to  $60^\circ$  in the excited state (Figure 9). The average Cu–N bond length decreases by 0.03 Å after photoexcitation. The use of an MO based approach to calculate XAFS spectra has allowed us to quantitatively analyze the XANES region and to give a simple interpretation to the first shoulder, P1, and corresponding peak of the difference spectrum. These results may be compared to

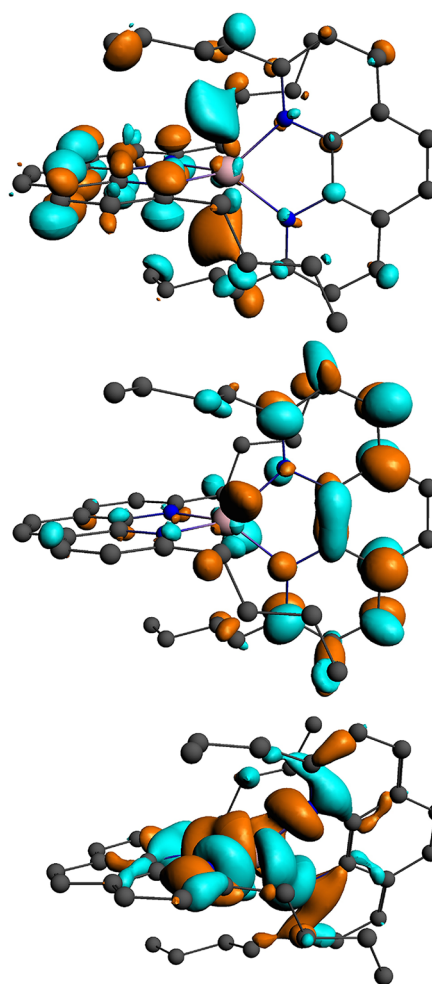


**Figure 8.** Molecular orbitals that contribute to the peak P1 of the  $[\text{Cu}^{\text{I}}(\text{dbp})_2]^+$  in the ground state (top and middle) and to the pre-edge peak at -7 eV of the flattened model of the excited state (bottom).

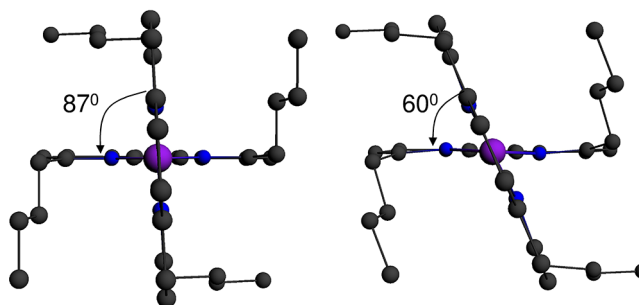


**Figure 9.** View of  $[\text{Cu}^{\text{I}}(\text{dbp})_2]^+$  in the ground (left) and  $^3\text{MLCT}$  (right) states showing the angular distortion.

those reported on  $[\text{Cu}(\text{R}_2\text{-phen})_2]^+$  ( $\text{R} = \text{Ph}$ <sup>38</sup>). In that case the feature on the rising edge of the absorption edge, which was assigned at due to the dipole allowed  $1s-4p_z$  transition, is more pronounced. The steric distortion in the ground state from a pseudotetrahedral geometry is greater in the ground state than in our example. The additional flattening in the  $^3\text{MLCT}$  states causes little or no increase in relative intensity of this peak, implying that the intensity may be due to additional multiple scattering components involving the phenyl substituents.

## CONCLUSIONS

In this study, we have shown that the energy dispersive XAS data acquisition is suited for fast time-resolved pump–probe experiments down to the ns time scale. The principle was demonstrated at ID24 of the European Radiation Facility, looking at the MLCT of  $[\text{Cu}(\text{R}_2\text{-phen})_2]^+$  excited state derivatives. Taken in conjunction with previous work, these results demonstrate that the lifetime of the emissive  $^3\text{MLCT}$  state can be increased by sterically bulky groups adjacent to the coordinated nitrogens by suppressing the formation of an exciplex and flattening by Jahn–Teller distortion.<sup>21,34,38</sup> The Cu K-edge XAS was obtained with a higher signal/noise and in a shorter acquisition time, as compared to step-by-step scanning approaches as reported in literature. Here a high quality spectrum was obtained in about 2 h; this was not limited by the detector, but was mainly due to the low repetition rate of the laser used (10 Hz) and dead-times in the experimental protocol. Upgrading to a kHz laser, as well as upgrades of the ESRF source (i.e., photon flux), should bring the overall acquisition time down to less than 2 min, using this energy dispersive data acquisition methodology. The XAS data acquisition time-resolution which can be obtained is limited to the bunch length of the synchrotron source, being  $\sim 70$  ps at the ESRF. Other (newer) sources like the Diamond Light source will be able to improve on this, with a source bunch length of  $\sim 40$  ps, in standard filling modes, and  $\sim 5$  ps in a low  $\alpha$ -mode.<sup>39</sup>

Fast acquisition (200 s integration time per X-ray energy point) has also been reported using a kHz laser and measuring time series XAFS spectra with a repetition rate of a 24 bunch mode at the APS (153 ns).<sup>40</sup> This has provided an efficient method of acquisition on a time scale of 100s ns to 1  $\mu\text{s}$  with a time resolution of 100 ps. By using an optimized laser repetition rate for the SLS (520 kHz), transient XAFS of MbCO (2 mM) have been obtained in  $\sim 4.5$  h.<sup>41</sup> The principal disadvantage of the dispersive approach is the restriction to a transmission geometry and thus this test experiment utilized relatively high concentrations (15–20 mM). However, this limitation is alleviated with highly stable X-ray sources, and thus the intrinsic gain by multiplexing the X-ray spectrum should still be a very significant real-time gain in kinetic studies of structural changes. These are being initiated at the Diamond Light Source (I20) and the ESRF (ID24).

## AUTHOR INFORMATION

### Corresponding Author

\*E-mail: (J.E.) je@soton.ac.uk.

### Notes

The authors declare no competing financial interest.

## ACKNOWLEDGMENTS

We thank EPSRC for funding (EP/I01974X/1) and access to the RCaH facilities. The ESRF is gratefully acknowledged for beamtime under project CH2849. M.T. gratefully acknowledges the EPSRC (EP/E060404/1) and G.S. funding from SNF (Grant No. 200021\_135226). The following people are gratefully acknowledged for their help and discussions before, during and/or after the experiment: Sofia Diaz-Moreno, Monica Amboage, Matthew Gerring, Janet Groves, Christine Mills, Florian Perrin, Marie Christine Dominguez, Sakura Pascarelli, Friederike Ewald, and Michael Wulff.

## REFERENCES

- (1) Ruthkosky, M.; Kelly, C. A.; Zaros, M. C.; Meyer, G. J. Long-Lived Charge-Separated Excitation of Cu(I) Donor-Acceptor Compounds. *J. Am. Chem. Soc.* **1997**, *119*, 12004–12005.
- (2) Thanasekaran, P.; Liao, R. T.; Liu, Y. H.; Rajendran, T.; Rajagopal, S.; Lu, K. L. Metal-Containing Molecular Rectangles: Synthesis and Photophysical Properties. *Coord. Chem. Rev.* **2005**, *249*, 1085–1110.
- (3) Vannelli, T. A.; Karpishin, T. B. Neocuproine-extended Porphyrin Coordination Complexes. 2. Spectroscopic Properties of the Metalloporphyrin Derivatives and Investigations into the HOMO Ordering. *Inorg. Chem.* **2000**, *39*, 340–347.
- (4) Armaroli, N.; Balzani, V.; Barigelletti, F.; Decola, L.; Flamigni, L.; Sauvage, J. P.; Hemmert, C. Supramolecular Photochemistry and Photophysics—a [3]-Catenand and its Mononuclear and Homodinuclear and Heterodinuclear [3]-Catenates. *J. Am. Chem. Soc.* **1994**, *116*, 5211–5217.
- (5) Collin, J. P.; Dietrich-Buchecker, C.; Gavina, P.; Jimenez-Molero, M. C.; Sauvage, J. P. Shuttles and Muscles: Linear Molecular Machines Based on Transition Metals. *Acc. Chem. Res.* **2001**, *34*, 477–487.
- (6) Sauvage, J.-P. Chemistry—A Light-Driven Linear Motor at the Molecular Level. *Science* **2001**, *291*, 2105–2106.
- (7) Cunningham, C. T.; Cunningham, K. L. H.; Michalec, J. F.; McMillin, D. R. Cooperative Substituent Effects on the Excited States of Copper Phenanthrolines. *Inorg. Chem.* **1999**, *38*, 4388–4392.
- (8) Kirchoff, J. R.; McMillin, D. R.; Robinson, W. R.; Powell, D. R.; McKenzie, A. T.; Chen, S. Steric Effects and the Behavior of  $\text{Cu}(\text{NN})(\text{PPh}_3)_2^+$  Systems in Fluid Solution—Crystal and Molecular Structures of  $[\text{Cu}(\text{dmp})(\text{PPh}_3)_2]\text{NO}_3$  and  $[\text{Cu}(\text{phen})(\text{PPh}_3)_2]\text{NO}_3 \cdot 1.5\text{EtOH}$ . *Inorg. Chem.* **1985**, *24*, 3928–3933.
- (9) Palmer, C. E. A.; McMillin, D. R. Singlets, Triplets and Exciplexes—Complex, Temperature-Dependent Emissions from  $\text{Cu}(\text{dmp})(\text{PPh}_3)_2^+$  and  $\text{Cu}(\text{phen})(\text{PPh}_3)_2^+$  in Solution. *Inorg. Chem.* **1987**, *26*, 3837–3840.
- (10) Berger, R. M.; McMillin, D. R.; Dallinger, R. F. Two-Photon Photochemistry of  $[\text{Cu}(\text{dmp})_2]^+$ . *Inorg. Chem.* **1987**, *26*, 3802–3805.
- (11) Blasse, G.; Breddels, P. A.; McMillin, D. R. The Luminescence of Solid Bis(2,9-diphenyl-1,10-phenanthroline) Copper(I). *Chem. Phys. Lett.* **1984**, *109*, 24–26.
- (12) Cunningham, K. L.; Hecker, C. R.; McMillin, D. R. Competitive Energy-Transfer and Reductive Quenching of the CT Excited States of Copper(I) Phenanthrolines. *Inorg. Chim. Acta* **1996**, *242*, 143–147.
- (13) Cunningham, C. T.; Moore, J. J.; Cunningham, K. L. H.; Fanwick, P. E.; McMillin, D. R. Structural and Photophysical Studies of the  $\text{Cu}(\text{NN})_2^+$  Systems in the Solid State. Emission at Last from Complexes with Simple Phenanthroline Ligands. *Inorg. Chem.* **2000**, *39*, 3638–3644.
- (14) Iwamura, M.; Watanabe, H.; Ishii, K.; Takeuchi, S.; Tahara, T. Coherent Nuclear Dynamics in Ultrafast Photoinduced Structural Change of Bis(diimine)copper(I) Complex. *J. Am. Chem. Soc.* **2011**, *133*, 7728–7736.
- (15) McMillin, D. R.; Kirchoff, J. R.; Goodwin, K. V. Exciplex Quenching of Photo-excited Copper-Complexes. *Coord. Chem. Rev.* **1985**, *64*, 83–92.
- (16) Armaroli, N. Photoactive Mono- and Polynuclear Cu(I) Phenanthrolines. A Viable Alternative to Ru(II)-Polypyridines. *Chem. Soc. Rev.* **2001**, *30*, 113–125.
- (17) Casadonte, D. J., Jr.; McMillin, D. R. Dual Emissions from  $\text{Cu}(\text{dmp})(\text{PR}_3)_2^+$  Systems in a Rigid Glass – Influence of the Phosphine Donor Strength. *Inorg. Chem.* **1987**, *26*, 3950–3952.
- (18) Ichinaga, A. K.; Kirchoff, J. R.; McMillin, D. R.; Dietrich-Buchecker, C. O.; Marnot, P. A.; Sauvage, J.-P. Charge-Transfer Absorption and Emission of  $\text{Cu}(\text{NN})_2^+$ . *Inorg. Chem.* **1987**, *26*, 4290–4292.
- (19) Blaskie, M. W.; McMillin, D. R. Photostudies of Copper(I) Systems. 6. Room Temperature Emission and Quenching Studies of  $[\text{Cu}(\text{dmp})_2]^+$ . *Inorg. Chem.* **1980**, *19*, 3519–3522.

- (20) Everly, R. M.; McMillin, D. R. Reinvestigation of the Absorbing and Emitting Charge-Transfer Excited-States of  $[\text{Cu}(\text{NN})_2]^+$  Systems. *J. Phys. Chem.* **1991**, *95*, 9071–9075.
- (21) Chen, L. X.; Shaw, G. B.; Novoyhilova, I.; Liu, T.; Jennings, G.; Attenkofer, K.; Meyer, G. J.; Coppens, P. MLCT State Structure and Dynamics of a Copper(I) Diimine Complex Characterized by Pump-Probe X-ray and Laser Spectroscopies and DFT Calculations. *J. Am. Chem. Soc.* **2003**, *125*, 7022–7034.
- (22) Shaw, G. B.; Grant, C. D.; Shiota, H.; Castner, E. W., Jr.; Mezer, G.; Chen, L. X. Ultrafast Structural Rearrangements in the MLCT Excited State for Copper(I) Bis-Phenanthrolines in Solution. *J. Am. Chem. Soc.* **2007**, *129*, 2147–2160.
- (23) Smolentsev, G.; Soldatov, A. V.; Chen, L. X. Three-Dimensional Local Structure of Photoexcited Cu Diimine Complex Refined by Quantitative EXAFS Analysis. *J. Phys. Chem. A* **2008**, *112*, 5363–5367.
- (24) Chen, L. X. Excited State Molecular Structure Determination in Disordered Media using Laser Pump/X-Ray Probe Time-Domain X-Ray Absorption Spectroscopy. *Faraday Discuss.* **2003**, *122*, 315–329.
- (25) Gawelda, W.; Pham, V. T.; Benfatto, M.; Zaushtsyn, Y.; Kaiser, M.; Grolimund, D.; Johnson, S. L.; Abela, R.; Hauser, A.; Bressler, C.; et al. Structural Determination of a Short-Lived Excited Iron(II) Complex by Picosecond X-Ray Absorption Spectroscopy. *Phys. Rev. Lett.* **2007**, *98*, 057401.
- (26) Bressler, C.; Chergui, M. Ultrafast X-Ray Absorption Spectroscopy. *Chem. Rev.* **2004**, *104*, 1781–1812.
- (27) Tromp, M.; van Berkel, S. S.; van den Hoogenband, A.; Feiters, M. C.; de Bruin, B.; Fiddy, S. G.; van Bokhoven, J. A.; van Leeuwen, P. W. N. M.; van Strijdonck, G. P. F.; Koningsberger, D. C. Multitechnique Approach to Reveal the Mechanism of Copper(II)-Catalyzed Arylation Reactions. *Organometallics* **2010**, *29*, 3085–3097.
- (28) Headspith, J.; Groves, J.; Luke, P. N.; Kogimtzis, M.; Salvini, G.; Thomas, S. L.; Farrow, R. C.; Evans, J.; Rayment, T.; Lee, J. S.; et al. First Experimental Data from XH, a Fine Pitch Germanium Microstrip Detector for Energy Dispersive EXAFS (EDE). *IEEE Nucl. Sci. Conf. Rec.* **2007**, *N55-2*, 2421–2428.
- (29) Mathon, O.; Baudelet, F.; Itié, J.-P.; Pasternak, S.; Polian, A.; Pascarelli, S. XMCD Under Pressure at the FeK Edge on the Energy-Dispersive Beamline of the ESRF. *J. Synchrotron Radiat.* **2004**, *11*, 423–427.
- (30) Guerra, C. F.; Snijders, J. G.; te Velde, G.; Baerends, E. J. Towards an Order-N DFT Method. *Theor. Chem. Acc.* **1998**, *99*, 391–403. Velde, G. T.; Bickelhaupt, F. M.; Baerends, E. J.; Guerra, C. F.; Van Gisbergen, S. J. A.; Snijders, J. G.; Ziegler, T. *J. Comput. Chem.* **2001**, *22*, 931–967.
- (31) Baerends, E. J.; Ellis, D. E.; Ros, P. Self-Consistent Molecular Hartree-Fock-Slater Calculations - I. The Computational Procedure. *Chem. Phys.* **1973**, *2*, 41–51.
- (32) Vosko, S. H.; Wilk, L.; Nusair, M. Accurate Spin-Dependent Electron Liquid Correlation Energies for Local Spin-Density Calculations - A Critical Analysis. *Can. J. Phys.* **1980**, *58*, 1200–1211.
- (33) Chen, L. X.; Zhang, X.; Lockard, L. V.; Stickrath, A. B.; Attenkofer, K.; Jennings, G.; Liu, D.-J. Excited-State Molecular Structures Captured by X-Ray Transient Absorption Spectroscopy: A Decade and Beyond. *Acta Crystallogr.* **2010**, *A66*, 240–251.
- (34) Gothard, N. A.; Mara, M. W.; Huang, J.; Szarko, J. M.; Rolczynski, B.; Lockard, J. V.; Chen, L. X. Strong Steric Hindrance Effect on Excited State Structural Dynamics of Cu(I) Diimine Complexes. *J. Phys. Chem. A* **2012**, *116*, 1984–1992.
- (35) Goodwin, K. V.; McMillin, D. R. Anion-Induced Quenching of Star-Cu(dmp)<sub>2</sub><sup>+</sup>. *Inorg. Chem.* **1987**, *26*, 875–877.
- (36) Everly, R. M.; McMillin, D. R. Concentration-Dependent Lifetimes of Cu(NN)<sub>2</sub><sup>+</sup> Systems—Exciplex Quenching from the Ion-Pair State. *Photochem. Photobiol.* **1989**, *50*, 711–716.
- (37) Kau, L. S.; Spira-Solomon, D. J.; Penner-Hahn, J. E.; Hodgson, K. O.; Solomon, E. I. X-Ray Absorption-Edge Determination of the Oxidation-State and Coordination-Number of Copper—Application to the Type-3 Site in Rhus-Vernicifera Laccase and its Reaction with Oxygen. *J. Am. Chem. Soc.* **1987**, *109*, 6433–6437.
- (38) Mara, M. W.; Jackson, N. E.; Huang, J.; Stickrath, A. B.; Zhang, X.; Gothard, N. A.; Ratner, M. A.; Chen, L. X. Effects of Electronic and Nuclear Interactions on the Excited-State Properties and Structural Dynamics of Copper(I) Diimine Complexes. *J. Phys. Chem. B* **2013**, *117*, 1921–1931.
- (39) Martin, I. P.S.; Rehm, G.; Thomas, C.; Bartolini, R. Experience with Low-alpha Lattices at the Diamond Light Source. *Phys. Rev. ST Accel. Beams* **2011**, *14*, 040705.
- (40) Lockard, J. V.; Rachford, A. A.; Smolentsev, G.; Stickrath, A. B.; Wang, X.; Zhang, X.; Attenkofer, K.; Jennings, G.; Soldatov, A.; Rheingold, A. L.; et al. Triplet Excited State Distortions in a Pyrazolate Bridged Platinum Dimer Measured by X-ray Transient Absorption Spectroscopy. *J. Phys. Chem.* **2010**, *114*, 12780–12787.
- (41) Lima, F. A.; Milne, C. J.; Amarasinghe, D. C. V.; Rittmann-Frank, M. H.; van der Veen, R. M.; Reinhard, M.; Pham, V.-T.; Karlsson, S.; Johnson, S. L.; Grolimund, D.; et al. A High-Repetition Rate Scheme for Synchrotron-Based Picosecond Laser Pump/X-ray Probe Experiments on Chemical and Biological Systems in Solution. *Rev. Sci. Instrum.* **2011**, *82*, 063111.